Comparison of quantum confinement effects between quantum wires and dots

Jingbo Li and Lin-Wang Wang [a)]

Computational Research Division,
Lawrence Berkeley National Laboratory, Berkeley, CA 94720

March 15, 2003

Abstract

Dimensionality is an important factor to govern the electronic structures of semiconductor nanocrystals. The quantum confinement energies in one-dimensional quantum wires and zero-dimensional quantum dots are quite different. Using large-scale first-principles calculations, we systematically study the electronic structures of semiconductor (including group IV, III-V, and II-VI) surface-passivated quantum wires and dots. The band-gap energies of quantum wires and dots have the same scaling with diameter for a given material. The ratio of band-gap-increases between quantum wires and dots is material-dependent, and slightly deviates from 0.586 predicted by effective-mass approximation. Highly linear polarization of photoluminescence in quantum wires is found. The degree of polarization decreases with the increasing temperature and size.

[a)] Email: lwwang@lbl.gov

1. Introduction

Semiconductor nanocrystals, such as quantum dots (QDs)[1] and quantum wires (QWs)[2] are of intense scientific and technological interest. Their electronic structures can be tailored by their sizes and shapes, leading to many new applications from lasers, [3] biological cell labelling, [4] to solar cells. [5] In comparison with QDs, the study of QWs has attracted less attention because of the technical difficulties to synthesis them. However, recently, high-quality semiconductor QWs can be fabricated by a solution-liquid-solid approach in wet chemistry. [4-9] The diameter of the QWs synthesized in this way is small enough to show strong quantum confinement effect just like in colloidal QDs. Then one natural task is to compare the quantum confinement effects in QWs and QDs for the same materials. This gives us a way to study the effects of dimensionality [9] in the quantum confinement systems.

According to simple effective-mass approximation model,[10-12] the band gap increases of QDs and QWs from the bulk value is $\Delta E_g = \frac{2\hbar^2\zeta^2}{m^* d^2}$, where $\frac{1}{m^*} = \frac{1}{m_e^*} + \frac{1}{m_h^*}$ (m_e^* and m_h^* are electron and hole's effective-mass, respectively), and d is the diameter. For spherical QDs, $\zeta = \pi$ is the zero point of the spherical Bessel function, while for cylindrical QWs, $\zeta = 2.4048$ is the zero point of the cylindrical Bessel function. Thus the ratio of band-gap-increases between the QW and QD should be $\Delta E_g^{wire} / \Delta E_g^{dot} = 0.586$. There are two questions about this simple effective mass model: (1) Does the ΔE_g follow the $1/d^2$ scaling? If not, do the QW and QD ΔE_g have the same scaling? (2) Is the real ratio $\Delta E_g^{wire} / \Delta E_g^{dot}$ close to 0.586 ?

These questions have been addressed in some degree by experiments for some particular systems like InP and CdSe. [6-8] Here, we like to address these questions from *ab initio* calculations for many more materials: Si, InP, InAs, GaAs, CdSe, CdS, and CdTe. Unlike the experiments where the exact diameters of the QD and QW always have some uncertainties due to size distribution, in our *ab initio* calculations, there is no such uncertainties.

To do *ab initio* calculations for thousand atom colloidal systems, we will use a recently developed charge patching method. This method has been applied successfully to calculate the electronic structure of unconventional semiconductor alloy with supercell containing 4096 atoms, [13-15] and IV-IV, III-V, II-VI thousand atom semiconductor QDs.[16] Before this method, empirical pseudopotential method (EPM) was used to calculate the electronic structure of semiconductor nanocrystals. [17,18] Compared to the EPM method, charge patching method has the following advantages: (1) There is no fitting uncertainties which exists in the EPM method. There is no fitting procedure in the charge patching method. The charge patching method generates the local-density approximation (LDA) quality charge density of a large nano-system without doing a self-consistent LDA calculation for the large system. (2) The surface passivation of a colloidal nanosystem is straight forward and physical. In EPM, it takes a long time to fit a surface passivation for a given material. Despite all these advantages, the charge patching method is relatively new, especially in its application to colloidal nanocrystals. Thus, the second task of this paper is to check the accuracy of this method, especially for the calculation of QWs.

2. Method

The calculation scheme for the charge patching method is the following. First we use pseudo-hydrogen atoms (with fractional nuclei charges and numbers of electrons) on the surface of QWs, which provides an ideal passivation to pair the electron in the dangling bonds. Second, we generate the *ab initio* quality electron charge density $\rho_{patch}(r)$ using charge motifs generated from prototype systems with similar atomic environments. Third, via the solution of Poisson's equation, the standard LDA formula can be used to calculate the total LDA potential *V(r)*. Then the single particle Schrodinger's (or Kohn-Sham's) equation $[-\frac{1}{2}\nabla^2 + V(r)]\Psi_i = \varepsilon_i \Psi_i$ can be solved using the linear scaling folded spectrum method (FSM) for the band edge states. [19] The FSM searches for the minimum of $\langle \Psi_i | (H - E_{ref})^2 | \Psi_i \rangle$, where E_{ref} is a reference energy placed inside the band gap. The details of this whole procedure are published in Ref. [16].

We have studied Si, GaAs, InAs, InP, CdSe, CdS, and CdTe QWs in [111] growth directions (we will also call it *c*-axis or *z*-direction in the following). We use the experimental bulk lattice constants shown in Table I. The effective diameter of QWs is defined in terms of the number of atoms N_{wire} in the wire (with one unit cell along [111] *c*-axis) as $d = a(\frac{\sqrt{3}}{4\pi} N_{wire})^{1/2}$, where *a* is the bulk lattice constant. We have used plane-wave basis sets and norm conserving pseudopotentials in our calculations. The kinetic energy cutoff for plane-wave basis set is listed in Table I. We found our calculated bulk band structures are in excellent agreement with all electron linearized augmented plane wave (LAPW) method results. [20] The real space grids for the largest quantum wire are 320×320×64.

3. Results and Discussion

We first test the accuracy of the charge patching method for QWs. The test is done by comparing the charge patching method calculated results with direct self-consistent LDA calculated results. We will test the calculated eigen energies and charge densities. We will use InP as our test case, although similar results are found for other systems. Fig. 1 plots the energy shifts of the conduction band minimum (CBM) and valence band maximum (VBM) states of InP QWs from the bulk values. The largest error (48 meV in CBM and 29 meV in VBM) are found in the QWs with diameter of 1.34 nm. After the size of QWs larger than 2 nm, the single particle eigen energies cause an error within 20 meV compared to direct LDA calculations. The errors of band gap ΔE_g shown in Table I are even smaller. The 1.34 nm QWs have 19 meV error. The QWs larger than 2 nm have typical errors of just ≤ 5 meV. The bulk InP has only 3×10^{-4} meV error in the gap, which can be thought as very large size QWs (diameter is infinite). The accuracy of the patched charge density $\rho_{patch}(r)$ itself can be measured by its difference to the directly calculated self-consistent LDA charge density $\rho_{LDA}(r)$: $\Delta\rho = \int\left|\rho_{patch}(r) - \rho_{LDA}(r)\right|d^3r \Big/ \int\rho_{LDA}(r)d^3r$. The results are shown in Table I for different systems. Overall, we get a charge density error less than *1%*, similar to what we get for semiconductor QDs. [16]

After established the accuracy of the charge patching method, we can now use it to study the electronic states of various QWs. In Fig. 2, we have shown the contour plots of charge density distribution for the CBM state and VBM state of a 5.2 nm diameter InP QW. The wave functions of both CBM and VBM states are distributed mostly in the interior of the wire rather than at the surface. The envelope functions of both CBM and VBM states are σ-type (*s*-like in the *xy* plane). The electronic band structure of InP QWs

with diameter of 5.18 nm is plotted in Fig. 3 (a). In the conduction band, the lowest energy state is σ_c, and the next energy state is π_c (*p*-like envelope function in the *xy* plane) with double degeneracy. The subscript *c* stands for the conduction band. In the valence band, the highest energy state is σ_z. Here, the subscript *z* indicates the Bloch part of the wave function has a p_z character. The next energy state is π_z with a double degeneracy. Lower than that, the energy states are π_{xy} with a double degeneracy. Here, the subscribe *xy* indicates the p_{xy} character of the Bloch part of the wave function.

The band gap change ΔE_g as a function of QW diameter is plotted in Fig. 3 (b). We fit ΔE_g with diameter *d* using an expression $\Delta E_g = \beta / d^{\alpha}$. We get α = 1.10972 for InP QWs. The quality of the fitting is shown in Fig.3(c). This α value we get is far away from the simple effective-mass value of α=2.

We have done the same fitting for the calculated QD band gaps. The fitted results of α and β are listed in Table III for all the systems we have calculated. By comparing the values between QD and QW, we have the following observations: (1) The difference of α between QD and QW for a same material is very small. Typically they are within *4%*, except for CdS and CdTe, there the difference is about *6~8%*. (2) For these small differences, there is no systematic trend. For example, one cannot say α from QW is larger or smaller than the QD. (3) Given the small differences and the lack of trend, one can assume that the difference of α between QW and QD is probably due to fluctuation of the fitting, thus they can be set as the same. Note that the differences of α between different materials are more robust. Roughly, the IV-IV material of Si has $\alpha \approx$ 1.6, while the III-V materials have $\alpha \approx$ 1.0, and the II-V materials have $\alpha \approx$ 1.2.

By assuming the α_{dot} to be the same as α_{wire}, we can use α_{dot} to fit the ΔE_g of the QWs. That gives us a new β'_{wire} which is also listed in Table III. As a result, the $\Delta E_g^{wire}(d)/\Delta E_g^{dot}(d)$ ratio will just be the ratio of $\beta'_{wire}/\beta_{dot}$. We found this ratio to range from 0.564 (for Si) to 0.731 (for CdS). All these ratios are relatively close to the simple effective mass results of 0.586, but in average they are slightly larger than the effective mass result.

Finally, to highline a difference of the QW electronic structure from the QD, we have calculated the photoluminescence (*PL*) polarization. One common characteristic of the QW PL spectra is that: the linear polarization along the *z*-direction and the *xy*-directions are significantly different. This can be used as an experimental indicator to distinguish the QWs from QDs. It also opens doors to new device applications such as polarization-sensitive nanoscale photodetectors, integrated photonic circuits, optical switches and interconnects. [21] However, the polarization might sensitively depend on the temperature, especially for large QW. To get this temperature dependence, we have calculated 40 conduction band states and 40 valence band states of a given QW for 100 k_z points. The optical transition matrix elements between these 40 states are calculated, and the Boltzmann distribution is used to occupy the states. The resulting PL polarization along *z* and *xy* directions are calculated for different temperatures for *d*=2.37 nm and *d*=5.37 nm CdSe QWs. The resulting linear polarization defined as $P = \frac{I_{\parallel} - I_{\perp}}{I_{\parallel} + I_{\perp}}$ [22] are shown in Fig.4. We find that for the small QW, the polarization is almost independent of

the temperature, while for the large QWs, the polarization is significantly reduced at room temperature from zero temperature result.

4. Conclusions

We have performed *ab initio* charge patching calculations for large-scale semiconductor QWs and confirmed its accuracy in thousand atom QWs applications. The present method is reliably applied to all the semiconductor systems without any fitting parameters. All the errors of eigen-energies compared with self-consistent LDA calculations are within 50 meV. Both the calculated QW and QD band gap can be described as a formula $\Delta E_g = \beta / d^{\alpha}$ with material-dependent parameters α and β. We find that for a given material, QWs and QDs have the same $1/d^{\alpha}$ scaling. But α is different from effective-mass value 2. The ratios of QW and QD band gap are also material-dependent, and range from 0.564 (for Si) to 0.731 (for CdS), slightly deviate from 0.586 predicted by effective-mass approximation. Finally, we have studied the linear polarization of PL in QWs. The degree of polarization decreases with the increasing temperature and size. But for small QWs, the degree of polarization is almost independent of temperature.

Acknowledgements

The authors thank Professor William E. Buhro for fruitful discussions. This work is supported by the U.S. Department of Energy, under Contract No. DE-AC03-76SF00098. This research used the resources of the National Energy Research Scientific Computing Center.

References

(1) Alivisatos, A. P. *Science* **1996**, *271*, 933.

(2) Xia, Y.; *et al*, *Adv. Mater.ature* **2003**, *15*, 353.

(3) Huang, M.; Mao, S.; Feick, H.; Yan, H.; Wu, Y.; Kind, H.; Weber, E.; Russo, R.; Yang, P., *Science* **2001**, *292*, 1897.

(4) Bruchez, M.; Moronne, M.; Gin, P.; Weiss, S.; Alivisatos, A. P. *Science* **1998**, *281*, 2013.

(5) Huynh, W. U.; Dittmer, J. J.; Alivisatos, A. P. *Science* **2002**, *295*, 2425.

(6) Yu, H.; Li, J.; Loomis, R. A.; Gibbons, P. C.; Wang, L. W.; Buhro, W. E., *J. Am. Chem. Soc.* **2003**, *125*, 16168.

(7) Yu, H.; Li, J.; Loomis, R. A.; Wang, L. W.; Buhro, W. E., *Nature Mater.* **2003**, *2*, 517.

(8) Duan, X.; Lieber, C. M. *Adv. Mater.* **2000**, *12*, 298.

(9) Kan, S.; Mokari, T.; Rothenberg, E.; Banin, U., *Nature Mater.* **2003**, *2*, 155.

(10) Zheng, W. H.; Xia, J. B.; Cheah, K. W., *J. Phys.: C* **1997**, *9*, 5105.

(11) Li, J.; Xia, J. B., *Phys. Rev. B* **2000**, *61*, 15880.

(12) Xia, J. B.; Li, J., *Phys. Rev. B* **1999**, *60*, 11540.

(13) Wang, L. W., *Phys. Rev. Lett.* **2002**, *88*, 256402.

(14) Li, J.; Wang, L. W., *Phys. Rev. B* **2003**, *67*, 205319.

(15) Li, J.; Wang, L. W., *Phys. Rev. B* **2003**, *67*, 033102.

(16) Wang, L. W.; Li, J., *Phys. Rev. B*, in press.

(17) Wang, L. W.; Zunger, A., *Phys. Rev. B* **1996**, *53*, 9579.

(18) Li, J.; Wang, L. W., *Nano Lett.* **2003**, *3*, 101; *Nano Lett.* **2003**, *3*, 1357; *Nano Lett.* **2004**, *4*, 29.

(19) Wang, L. W.; Zunger, A., *J. Phys. Chem. B* **1998**, *102*, 6449.

(20) Wei, S. H.; Zunger, A., *Phys. Rev. B* **1999**, *60*, 5404.

(21) Wang, J. F.; Gudiksen, M. S.; Duan, X.; Cui, Y.; Lieber, C. M., *Science* **2001**, *293*, 1455.

(22) Li, X. Z.; Xia, J. B., *Phys. Rev. B* **2002**, *66*, 115316.

Figure Captions

Fig. 1 The CBM and VBM band energy shifts of InP QWs from the bulk values. The full-squares correspond to the results of charge patching method. The LDA self-consistent calculations are shown as open-dots.

Fig. 2 Contour plot of charge density distribution of (a) CBM and (b) VBM state of InP QWs in *xz*-plane; and (c) CBM and (d) VBM in *xy*-plane. Magenta dots represent In-atom, yellow dots represent P-atom. The surface atoms are not ploted in this figure. Red, yellow, green, and blue colors indicate electron density from higher to lower.

Fig. 3 (a) Electronic band structure of InP QWs with diameter of 5.18 nm. The numbers in parentheses indicate the degeneracy of the states. (b) The change of the band gap ΔE_g as functions of the diameter *d* of the InP QWs. (c) The linear least-squares fit to ΔE_g vs $d^{-1.10972}$ for InP QWs.

Fig. 4. Degrees fo linear polarization as functions of temperature for CdSe QWs with diameter of 2.37nm and 5.37nm.

Tables

TABLE I. Zinc-blende lattice *a* (in Å) and kinetic energy cutoff (in Ryd) for the plane-wave basis set are used in this calculations.

	Si	GaAs	InAs	InP	CdSe	CdS	CdTe
a (Å)	5.43	5.65	6.06	5.87	6.08	5.82	6.48
E_{cut} (Ryd)	25.0	25.0	25.0	25.0	35.0	25.0	25.0

TABLE II. The accuracy of the charge patching method compared to direct self-consistent LDA calculations. The band gap errors for all eigenstates of other materials are similar to the band gap errors shown here.

system	$\Delta\rho$	ΔE_g (meV)
InP(bulk)	0.067%	3×10^{-4}
InP(100)	0.32%	18
InP(111)	0.39%	22
InP(110)	0.33%	15
d=1.34 nm	0.97%	19
d=2.29 nm	0.72%	1
d=2.84 nm	0.62%	3

TABLE III. The α and β for the β/d^{α} fit of the ΔE_g for different materials. The unit of β is eV×(nm)$^{\alpha}$. The QDs parameters of β_{dot} and α_{dot} are reported in Ref. [16]. We list here for comparison with these of QWs. Using α_{dot} to fit the ΔE_g of QWs, we get β'_{wire}.

	Si	GaAs	InAs	InP	CdSe	CdS	CdTe
β_{dot}	3.81	3.88	4.41	3.90	3.84	3.35	4.40
α_{dot}	1.60	1.01	1.01	1.10	1.18	1.22	1.28
β_{wire}	2.09	2.65	3.15	2.77	2.79	2.56	2.80
α_{wire}	1.53	0.97	0.98	1.11	1.20	1.30	1.18
β'_{wire}	2.15	2.64	3.22	2.76	2.79	2.45	2.83
$\beta'_{wire}/\beta_{dot}$	0.564	0.680	0.730	0.707	0.727	0.731	0.643

Fig. 1 Li and Wang

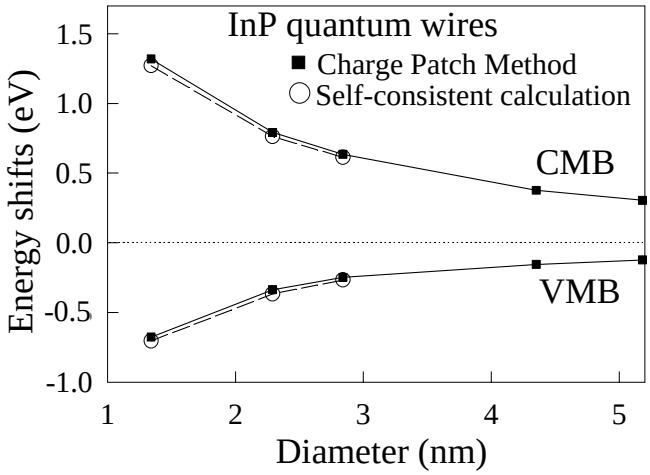

Fig. 2 Li and Wang

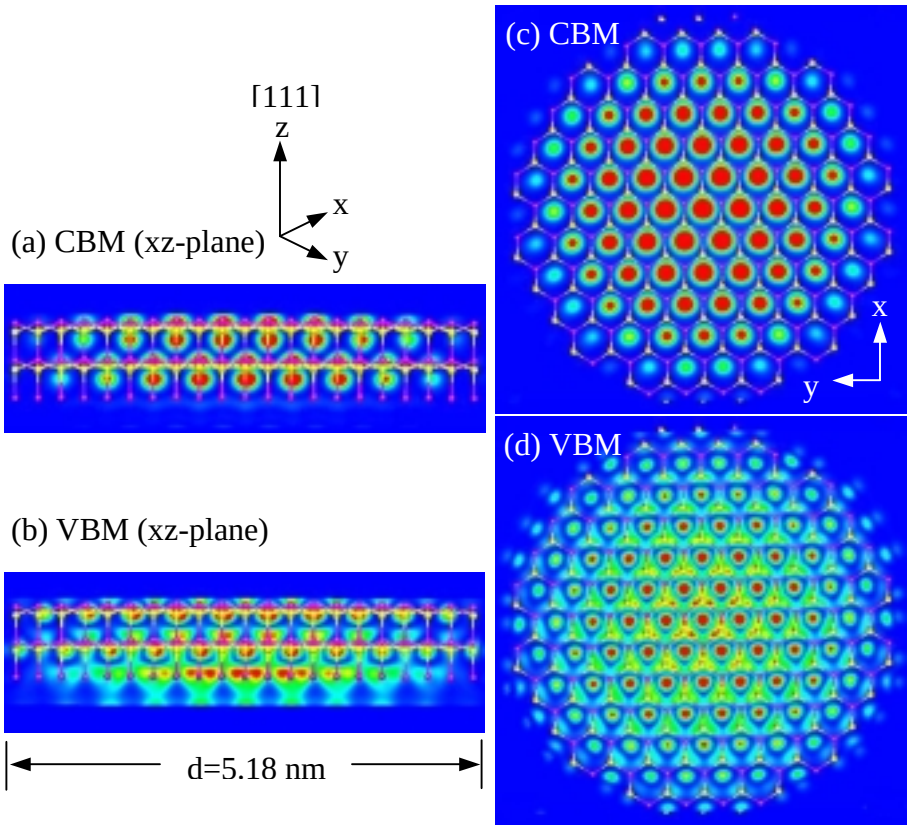

Fig. 3 Li and Wang

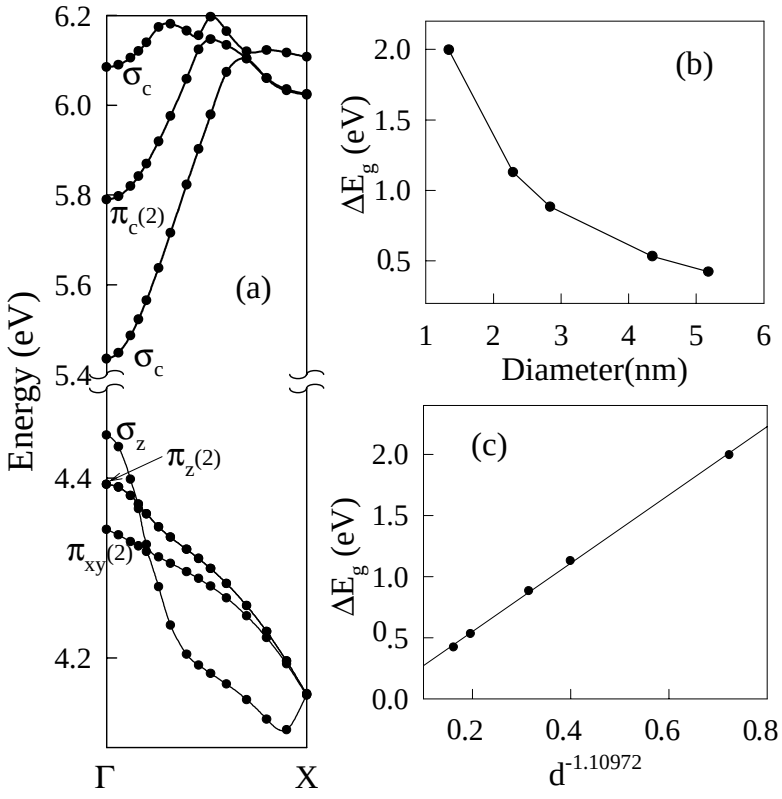

Fig. 4 Li and Wang